© APR 2026 | IRE Journals | Volume 9 Issue 10 | ISSN: 2456-8880
DOI: https://doi.org/10.64388/IREV9I10-1717141

X-Ray Photoelectron Spectroscopy (XPS) Spectra Characterization of Mild Steel Corrosion in Carbon Dioxide (CO_2) Deaerated Environment.

IKEH LESOR
University of Port Harcourt, Faculty of Engineering, Department of Petroleum and Gas Engineering, East-West Road, Choba, Port Harcourt, Nigeria, Choba.

Abstract- ***Corrosion of pipeline remain a major challenge in the oil and gas industry. Corrosion in oil and gas pipelines is an electrochemical process causing significant material degradation, leading to leaks, ruptures, and, on average, 50%–70% of pipeline failures. It is driven by environmental factors or contaminants such as CO2, H2S and water. Internal corrosion slows or decreases the production of oil and gas when associated with free water and reacts with organic acid. The aim of this study is to characterize the corrosion of carbon steel and surface film composition in well deaerated environment (3.5 wt. % Nacl) using the X-Ray Photoelectron Spectroscopy (XPS). The XPS characterization focused on identifying the chemical states of Fe, O, and C on the surface, revealing that corrosion products were primarily composed of a FeCO3 film, with traces of iron oxides (FeO), or (FeOOH). The results shows that the XPS analyses on the samples reviewed some of the elements are absence on addition of HAc to the solution. The Fe 2p spectra shows peaks corresponding to metallic iron, (FeO) from the substrate and Fe2+ and Fe3+ states from the corrosion products with Fe2+ in FeCO3 being dorminant in the passive film. Similarly, A prominent peak at approximately 290.5 eV, characteristic of the carbonate ion, CO32- in FeCO3 confirmed the formation of iron carbonate.The oxygen spectra were deconvoluted into multiple states, highlighting the presence of O2- and CO32-***

Keywords:X-Ray, Spectra, Carbon Steel, Corrosion, Environment, Spectroscopy, Photoelectron.

I. INTRODUCTION

Carbon dioxide (CO2) corrosion is a great concern in the oil industry. It results from the practice of pumping CO2-saturated water into wells to enhance oil recovery and reduce the viscosity of the pumped fluid. The presence of carbon dioxide in solution, however, leads to the formation of a weak carbonic acid (H2CO3) which drives CO2 corrosion reactions. In the process of oil and gas production, the aqueous phase present in hydrocarbon streams stands out as a significant contributor to the corrosion of pipelines and associated equipment. This issue is notably compounded when hydrogen sulfide (H2S) and carbon dioxide (CO2) are dissolved within the aqueous phase, thereby fostering an environment that is highly conducive to corrosion.

X-ray photoelectron spectroscopy (XPS) is the ideal tool to characterize CO2 corrosion and its decomposition reactions because it provides chemical state information from the top 2 nanometers of a specimen. The technique involves detecting photoelectrons emitted by the absorption of x-rays incident on the specimen. An incident x-ray transfers all its energy (hν) to an inner shell electron such that the kinetic energy of the emitted photoelectron is equal to that of the x-ray minus the binding energy of the electron. Small shifts in the measured kinetic energy of the photoelectron of 1–10 eV indicate changes in the binding energy and hence the local chemical state. All elements can be detected by XPS with the exception of hydrogen and helium due to their extremely low photoelectron generation cross sections (Heuer et al).

XPS is a valuable tool in identifying iron carbonate films on specimens exposed to CO2 corrosion because of its ability to distinguish chemical states. The binding energies for CO2 corrosion, however, have not been systematically characterized, and this is necessary to identify corrosion using XPS. This study therefore aim to examine the application of XPS to characterize CO2 corrosion of carbon steel in well deaerated environment.

© APR 2026 | IRE Journals | Volume 9 Issue 10 | ISSN: 2456-8880
DOI: https://doi.org/10.64388/IREV9I10-1717141

1.1 Assessment of corrosion failure in industry

Corrosion can impose a significant cost penalty on the choice of material at the design stage, and its possible occurrence also has serious safety and environmental implications (Kermani et al). A corrosion failure can also have a very serious impact on the environment. In the offshore oil industry, leakage from subsea oil well tubulars and transmission pipelines or the storage vessels and other equipment on offshore platforms poses the threat of pollution to the sea.

Table 1: Analysis of a selected number of failures in petroleum industries
(Kermani et al.)

Types of Failure	Frequency (%)
Corrosion (all types)	33
Fatigue	18
Mechanical damage/overload	14
Brittle fracture	9
Fabrication defects	9
(excluding weld defects) Welding defects	7
Others	10

When it comes directly from the well, the fluid is usually unprocessed and multiphase and can be a mixture of oil, solids, gas and water. The presence of water leads to considerable corrosion problems on the internal walls of the pipelines. The liquid can contain corrosive species such as organic acids and dissolved corrosive gases such as carbon dioxide (CO2) or hydrogen sulphide (H2S). Therefore the presence of these gases can lead to a very corrosion environment.

The carbon dioxide (CO2) corrosion or sweet corrosion has been known for a long time and continues to be a problem in the oil and gas industry, costing billions of dollars every year (Schmitt et al). The CO2 is present in oil phase with water as a dissolved gas under high pressures commonly found in underground oil and gas reservoirs. In the dissolved state, it forms carbonic acid as is shown in equation (1).

$$CO_2 + H_2O \leftrightarrow H_2CO_3 \quad (1)$$

The pipeline costs are considerable part of the investment in subsea projects. For long- distance, large-diameter pipelines, they can become prohibitively high if the corrosively of the fluid necessitates the use of corrosion-resistant alloys instead of carbon steel [Roberge P.R]. Therefore, better understanding and control of the corrosion of carbon steel can increase its application range and have a large economic impact.

Mild steel is used as the primary construction material for pipeline in oil and gas industry due to its low cost and availability. However, it is very susceptible to corrosion in CO2 environments. Carbon dioxide corrosion has been of interest to many researchers [Kermani et al, Nesic et al.] in the oil and gas industry for many years and there exists many theories about the mechanism of CO2 corrosion [Venkatraman et al]. Similarly, there has been a great interest in understanding the effect of different factors on the mechanism of CO2 corrosion and formation of iron carbonate film at the surface of the carbon steel because of the resulting corrosion rate.

Acetic acids (HAc) have been regarded as a source of hydrogen ions in its dissociation, increasing the acidification of the environment and the dissolution of the steel that leads to an increase in carbon steel corrosion rates, especially at low pH values. The acetic acid is the most common organic acid in multiphase systems containing brine [Gunaltun et al]. The acetic acids content in oil wells plays a determining role in the severity of corrosion rate even when only small concentrations are present [Anderson et al].

The precipitation of iron carbonate (FeCO3) is an importance process for corrosion control in the oil industry. The precipitated corrosion film of FeCO3 forms a layer of impermeable corrosion product which retards the corrosion process and lowers the corrosion rate by diffusion control. The formation of FeCO3 plays an important role in the formation of protective layers [Nafday et al]. When corrosion

© APR 2026 | IRE Journals | Volume 9 Issue 10 | ISSN: 2456-8880
DOI: https://doi.org/10.64388/IREV9I10-1717141

products are not deposited on the steel surface, very high corrosion rates of several millimeters per year can occur. The corrosion rate can be reduced substantially under conditions where FeCO3 can precipitate on the steel surface and form a dense and protective corrosion product film. This occurs more easily at high temperature or high pH in the water phase. When hydrogen sulphide (H2S) is present in addition to CO2, iron sulphide (Fes) films are formed rather than FeCO3 and protective films can be formed at lower temperature.

Corrosion inhibitor is one of the numerous methods used to protect against the corrosion process in the oil and gas industry. The inhibitors are commonly used to slow down corrosion process of mild steel in oilfield environment [Abayarathna]. The inhibitors can reduce corrosion of metal by forming a protective film that can isolate the metal from the aqueous corrosion environment. Water soluble and oil soluble inhibitors are the most commonly used in the oil and gas industry [Gulbrandsen et al.].

1.2 Thermodynamic aspects of aqueous corrosion

In electrochemistry, thermodynamic considerations help us to understand under which conditions a corrosion reaction is possible. Even though the corrosion rates cannot be obtained yet, it is necessary to analyze thermodynamic stability of each specific metal- electrolyte interface [Schmitt et al]

Now considering a corrosion reaction processes of iron in acidic media as shown in equation (2) to equation (4),

$$Fe + 2Hcl \leftrightarrow FeCl_2 + H_2 \quad (2)$$

At the anode, $Fe \rightarrow Fe^{2+} + 2e^- \quad (3)$

At the cathode, $2H^+ + 2e^- \rightarrow H_2 \quad (4)$

Both anodic and the cathodic partial reaction take place at the same electrode, which means both partial reactions cannot be separated and therefore no external voltage difference can be measured.In this present study, the thermodynamic stability of 3.5% wt. NaCl solution and HAc will be considered and used to characterize CO2 corrosion of mild steel in saturated brine environment using XPS analysis.

II. CO2 CORROSION PREDICTION MODELS

Corrosion of pipelines in multiphase flow is one of the complex problems facing the oil and gas industries. Several studies have significantly contributed to development of CO2 corrosion models. The models include:

2.1 Mechanistic model

The mechanistic models provide mathematical formulations of the chemical and electrochemical phenomena of the corrosion using mass, energy and charge balances. In an aqueous CO2 system, the processes commonly modelled by mechanistic approach include the electrochemical reactions at the surface along with the transport processes of species in the system.

$$H^+ + e^- \rightarrow \frac{1}{2}H_2 \quad (5)$$

$$H_2CO_3 + e^- \rightarrow \frac{1}{2}H_2 + HCO_3^- \quad (6)$$

$$HA_c + e^- \rightarrow \frac{1}{2}H_2 + Ac^- \quad (7)$$

This involves iron (Fe2+) dissolution, hydrogen ion (H+) reduction, carbon dioxide (CO2) dissolution, and carbonic acid (H2CO3) formation and reduction.

2.2 Semi-empirical model

The semi-empirical models are presented to resemble some of the physical principle of real system. The unknown parameters in the model are fitted in order to reproduce measured experimental corrosion data. The model is simple and can be evaluated easily. De Waard and Milliams developed a semi – empirical model from their corrosion experiments using the weight loss coupons and linear polarization experiments. The model is based on the assumption of direct reduction of H2CO3, and compared with correlation for the corrosion rate as a function of the partial pressure of CO2 and temperature in glass cell laboratory data as shown in equation (8):

$$\log V_{corr} = 7.96 - \frac{2320}{T + 273} - 5.55 \times 10^{-3}T + 0.67 \log \rho CO_2 \quad (8)$$

Where,

VCorr is the corrosion rate (mm/yr), T is the temperature (oC) and pCO2 is the CO2 partial pressure (bar).

The constant 0.67 in equation (…) was obtained by assuming that the pH is a function of pCO 2 only. The temperature functions was obtained by assuming arrhenius-type dependence for a charge transfer controlled process. They also assumed that the anodic process of iron dissolution proceeds via a pH-dependent mechanism. The scope of de Waard and Milliams model was revised on several occasions to extend its validity into areas where protective scales form and to account for high pH in brines, velocity, water. Despite all the theoretical shortcomings, the model of de Waard and Milliams et al stood as one of the important reference points for CO2 corrosion research over the past two decades, and in its most recently revised form [Waard and Williams], is still used as an informal industrial standard.

2.3 Empirical model

Empirical models are correlation of measured corrosion rate in mm/yr to a number of input variables. Example of the empirical models was presented by Halvorsen et al written as:

$$C\,R=K_T f_{CO2}^{0.6} \left(\frac{S}{19}\right)^{0.15+0.03\log f_0 \rho C\,O2} \quad (9)$$

Where,

CR = Corrosion rate, mm/yr; KT = Constant;

ρ C O2= Partial pressure of CO2, bar

S = Wall shear stress, pS

f = factor depending on CO2

2.4 Norsok CO2 corrosion model

The NORSOK M- 506 model is a pure empirical model based on laboratory data from single phase flow loops. It is an empirical corrosion rate model for carbon steel in water con taining CO2 at different temperatures, pH, CO2 partial pressure, and wall shear stresses. According to Norsok, CO2 corrosion within temperature range of 20oC to 120oC can be calculated using the empirical equation as:

$$C\,R=K_t \times f\,C\,O_2^{0.62} \left(\frac{S}{19}\right)^{0.146+0.0324\log f_0 f_{CO\,2}} \times f(\mathrm{p}\,H) \quad (10)$$

Where

Kt is a temperature–related constant, given in for a temperature range of 5oC to 150oC.

f (pH) is a factor depending on the pH of the solution. The Norsok primarily is meant as a guidance tool for material selection and for determination of the required corrosion allowance. The model is mainly made for pipelines systems where pure CO2 corrosion is the dominating corrosion reaction.

2.5 XPS Characterization

The X-ray photoelectron spectroscopy is a technique used to determine composition based on the photoelectric effect. Basically, it's an instrument used for investigating the surface chemistry of electrically conducting and non-conducting coupons. The XPS is viewed as a quantitative spectroscopic approach that provides information regarding the elemental composition in parts per thousand levels, based on the elemental electronic and chemical state of the electrode surface. It can measure the elemental composition, empirical formula, chemical state and electronic state of the elements within a material. Different reports have been presented on the use of XPS especially in the study of corrosion. Qiu et al uses the XPS for surface composition characterization and corrosion product analysis on carbon steel exposed to sea water. Qualitative analysis of surface films and formation of iron carbonate on carbon steel surfaces had also been studied using the XPS. Similarly Galicia et al uses the XPS to studied 1018 carbon steel surface composition exposed to alkaline medium as a function of immersion time and confirmed film formation on the steel surface. Ochoa et al uses the XPS to studied the formation and quantitative analysis of iron carbonate at carbon steel in respect to the structure of the carbon steel. The physical principle of the XPS is based upon a single photon in/electron out process. The energy of a photon of electromagnetic radiation is based on the Einstein equation given as in equation below

$$E=h\,v \quad (11)$$

© APR 2026 | IRE Journals | Volume 9 Issue 10 | ISSN: 2456-8880
DOI: https://doi.org/10.64388/IREV9I10-1717141

Where,

H is the planck constant (6.6210-34 Js) V is the frequency of the radiation (Hz)

The Axis Ultra DLD spectrometer Karros, (uses a monochromatic Al Kα X-ray source (1486.6 eV, 10 mA emission), and uses a delay line detector that enables fast acquisition of a narrow binding energy region which is used for sample position optimization (using a pertinent core level photoelectron peak). An electromagnetic in the analysis chamber below the sample position is used to incre ase the yield of photoelectrons reaching the analyzer slits. A charge neutralizer was used to compensate for any differential charging or, e.g., any poor connections between the sample

and sample plate (and thus ground). Survey spectra of a wide binding energy region were acquired with pass energy of 80 eV while high-resolution narrow scans of the important atomic core levels were acquired using a pass energy of 20 eV. The experiments were performed under high vacuum at pressures < 3 x 10-8 mbar. Data were analyzed using CASAXPS (www.casaxps.com), where photoelectron peaks are typically fit with product-approximation Voigt functions (Gaussian-Lorenztian peaks with a mixing ratio of 0.3).

III. METHODS AND PROCEDURE

The experiments in this study were carried out in a bubble cell glass beaker set-up connected with corrosion monitoring systems (linear polarization resistance LPR, potentiodynamic polarization PDP, and electrochemical impedance spectrum, EIS). The surface analyses was studied using the X-ray photoelectron spectroscope (XPS) to monitor and characterized the surface of the samples prior to and after every experiments. All experiments were conducted in a simulated artificial sea water (3.5% wt NaCl) solution saturated with CO2, and varies conditions of temperatures, 0.5 bar of partial pressure and pH of 6.0. The sample was positioned in a suitable evacuated housing an electron energy analyzer and a detector/data system analysis. This was however done in order to record the binding energy positions to the order of ±0.1 eV, and also to resolve photoelectron energies to better than 1 eV.

IV. RESULTS AND DISCUSSION

The XPS measurement technique was employed to analyse the composition of the organic absorbed layer on the surface of the carbon steel sample after exposure to different conditions. As a result, the high resolution peaks for O 1s, C 1s, N 1s, Fe 2p and Cl 2p for carbon steel surface after 6 hours of immersion in 3.5% wt. NaCl solution containing HAc, MEG and inhibitors are shown. All XPS spectra were observed to contained complex forms which were assigned to the corresponding species through a deconvolution fitting procedure using the CasaXPS facility.

4.1 O 1s spectra

The XPS spectra corresponding to the O 1s region for different test conditions and at different sputtering times are shown in Figure 1. In Figure 1, it is seen that only one single peak are observed at binding energy of 530 eV. This peak is corresponds to the hydroxyl groupings that results in the chemisorption of water and oxygen. The trend regarding the chemical nature of the species present in the corroded sample layer are the same in all the cases examined Similarly, Figure 1 shows that deconvolution of the O 1s spectrum main contributions are from oxygen in the form of oxide and anhydrous ions oxides (O2- and OH-). These results confirmed that the use of XPS for the identification of different types of oxidized iron species is complex because the core Fe2p region shows a little difference between iron compounds.

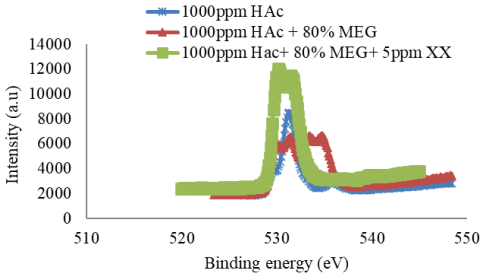

Figure 1: The XPS deconvolution profiles for O 1s for carbon steel in 3.5% wt. NaCl solution containing HAc, MEG and inhibitors.

© APR 2026 | IRE Journals | Volume 9 Issue 10 | ISSN: 2456-8880
DOI: https://doi.org/10.64388/IREV9I10-1717141

4.2 C 1s spectra

The XPS high resolution C 1s spectrum obtained on the carbon steel sample immersed in 3.5% wt. NaCl solution are presented in Figure 2 and Figure 3. The deconvolution of the C 1s and all other spectra was carried out with aid of CasaXPS software. In Figure 2 and Figure 3, it is seen that two peaks, the first peak at 285 eV and the second peak at 290 eV were identified. The first peak at 285 eV is considered as a result of aromatic or aliphatic carbon atoms together with the carbon atoms of the same type (C-C). The second peak at 290

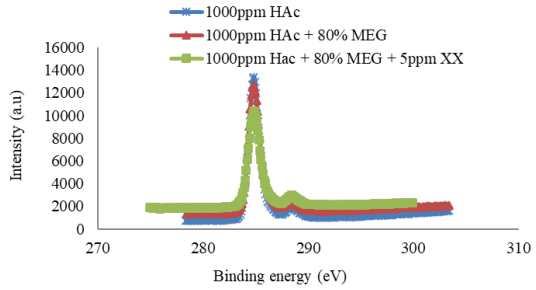

Figure 2: The XPS deconvolution profiles for C 1s for carbon steel in 3.5% wt. NaCl solution containing HAc, MEG and inhibitors

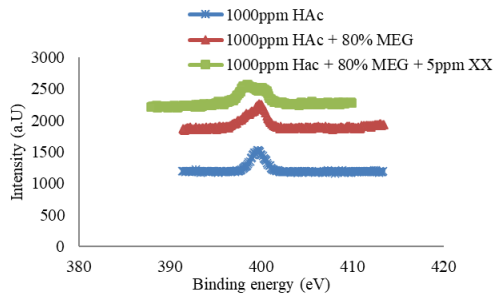

Figure 3: The XPS deconvolution profiles for N 1s for carbon steel in 3.5% wt. NaCl solution containing HAc, MEG and inhibitors

4.3 N 1s spectra

The XPS spectrum for N 1s has one single peak at approximately 400 eV as presented in Figure 4. This peak is shifted from 398 eV, the characteristic elemental binding energy of N 1s electron. This change in binding energy may due to the presence of Fe (III) and Zn (II). It is noted that the N 1s peak observed at 399.7 eV could be as a result of presence of (=N-) in the molecule absorbed on the electrode surface. However, the peak at 399.9 eV could be attributed to the neutral imine (-N+) and amine (-N-M) nitrogen atoms.

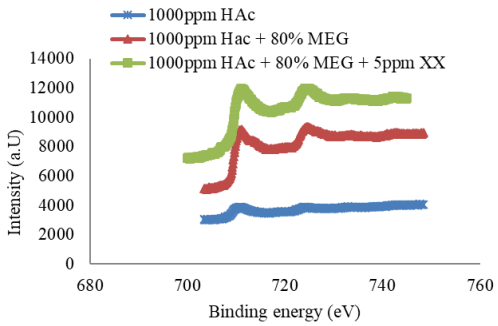

Figure 4: The XPS deconvolution profiles for Fe 2p for carbon steel in 3.5% wt. NaCl solution containing HAc, MEG and inhibitors

4.4 Fe 2p spectra

The XPS high resolution spectrum for Fe 2p3/2 is shown in Figure 5. It is noted that deconvolution of the spectrum suggests that two peaks are noticed corresponding to the metallic iron at 710 eV and 730 eV binding energy respectively. The first peak of Fe 2p corresponding to binding energy of 710 eV indicates for the resolution of chemical state of Fe2+ in the surface of the electrode materials, while the second peak at 730 eV corresponds to the formation of ferric surface oxidation products of Fe3+. The increase of peaks from 710 eV to 730 eV signifies that iron is present in Fe3+ state in the electrode surface film. The peak value at 711.0 eV is due to the presence of FeOOH and Fe (OH)3. This peak corresponds to the mean binding energy of Fe 2p in α-FeOOH as 711.0 ± 0.2 eV. The Fe 2p peak values with inhibitors are 711 eV and 725 eV. The peaks value noticed with the presence of inhibitors confirm the presence of Fe2O3, Fe3O4 and FeOOH and Fe3+ on the surface electrode. The film form with the inhibitors is seen as no protective.

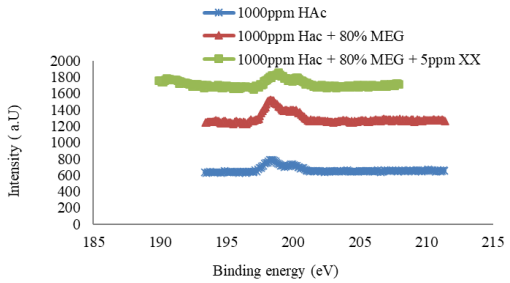

© APR 2026 | IRE Journals | Volume 9 Issue 10 | ISSN: 2456-8880
DOI: https://doi.org/10.64388/IREV9I10-1717141

Figure 5: The XPS deconvolution profiles for Cl 1s for carbon steel in 3.5% wt. NaCl solution containing HAc, MEG and inhibitors.

Table 2: Atomic percentage of XPS deconvolution profiles for carbon steel in 3.5% wt. NaCl solution containing HAc, MEG and inhibitors

Sample	C %	Cl %	Cu %	Fe %	N %	Na %	Ni %	O %	Total
HAc	74.70	0.56	0.28	0.65	1.39	3.58	0.40	18.84	100.00
HAc + MEG	64.25	0.96	1.48	2.94	1.76	0.02	0.66	28.05	100.00
HAc+MEG+Inhibitors	55.40	0.68	2.82	3.51	2.16	0.03	2.36	33.07	100.00

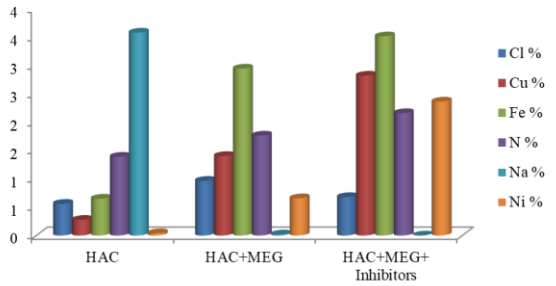

Figure 6: Variation of the XPS deconvolution profiles for carbon steel in 3.5% wt. NaCl solution containing HAc, MEG and inhibitors.

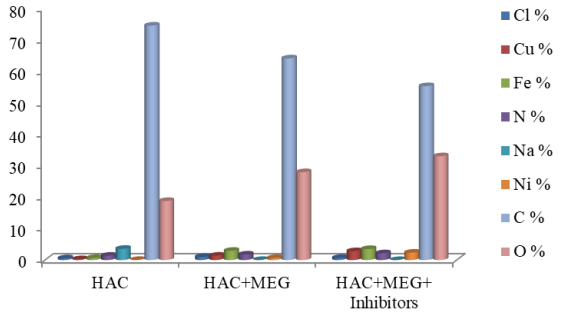

Figure 7: Variation of the XPS deconvolution profiles for carbon steel in 3.5% wt. NaCl solution containing HAc, MEG and inhibitors with C % and O %.

V. CONCLUSIONS

A comprehensive study on the characterization of carbon steel corrosion in deaearated environment at varies conditions had been carry out in this work using X-Ray Photoelectron Spectroscopy, (XPS). Based on the results obtained from the chemical composition, structure, and mechanism of the corrosion product layers, the following conclusions can be deducted:

- The analysis indicates that in deaerated CO2 environments, the initial corrosion product, which provides a level of passivity, is not exclusively an oxide but a mix of iron carbonate and hydrated iron oxides, with the protectiveness highly dependent on the stability and density of the FeCO3 formed.
- The XPS analysis confirms that the primary corrosion productin CO2 deaerated environment is iron carbonate, identified by the Fe 2p and C 1s peaks corresponding to Fe2+ and carbonate bonds
- In addition to iron carbonate form, a non-dissolved cementite from the sample matrix is identified on the surface of the sample especially, when the iron matrix dissolves faster than the carbides.

VI. ACKNOWLEDGEMENT

The authors would like to express their appreciation to the technical staff of the University of Salford, Manchester and the Department of Petroleum and Gas Engineering, University of Port Harcourt, for their support throughout the period of this work.

REFERENCES

[1] G.H.Koch, M.P.H.B., N.G.Thompson,Y.P.Virmani, and J.H.Payer, Corrosion Cost and Preventon Strategies in the United States. Federal highway administration, U.S. Department of Transportation: McLean VA., 2002.

[2] Kermani, M.B. and D. Harrop, The Impact of Corrosion on Oil and Gas Industry.

[3] Schmitt, G. and M. Horstemeier, Fundamental Aspects of CO2 Metal Loss Corrosion

a. Part II: Influence of Different Parameters on CO2 Corrosion Mechanisms. 2015, NACE International.

[4] Roberge, P.R., Corrosion basics: An introduction. 2006, NACE Press Book. p. 56-70.

[5] Nešić, S., Carbon Dioxide Corrosion of Mild Steel, in Uhlig's Corrosion Handbook. 2011, John Wiley & Sons, Inc. p. 229-245.

[6] Venkatraman, M.S., et al. Modeling corrosion of a metal under an aerosol droplet. in

[7] Materials Science Forum. 2010. Trans Tech Publications.

[8] Gunaltun, Y. and L. Payne, A New Technique for the Control of Top of the Line Cor- rosion: TLCC-PIG. NACE International.

[9] Abayarathna, D., A. Naraghi, and N. Obeyesekere, Inhibition of Corrosion of Carbon Steel in the Presence of CO2, H2S and S. NACE International.

[10] Gulbrandsen, E., et al., Effect of Precorrosion on the Performance of Inhibitors for CO2 Corrosion of Carbon Steel. NACE International.

[11] Pourbaix, M., Atlas of electrochemical equilibria in aqueous solutions. 1974: National Association of Corrosion Engineers.

[12] Vanloon, G.D., S, Environmental chemistry - a global perspective. 2011, Oxford University Press. p. 235-248.

[13] Bardal, E., Corrosion and Protection. 2004: Springer.

[14] Tait, W.S., An Introduction to electrochemical corrosion testing for practicing engi- neers and scientists. 1994, Pair Docs Publications.

[15] C.A Barlow, J., The Electrical Double Layer in physical chemistry: An Advanced Treatise, in Electrochemistry. 1970, Academic press, New York.

[16] T.Erdey-Gruz, Kinetics of Electrode Processes, in Wiley Interscience. 1972, John Wi- ley & Sons Inc, New York.

[17] Burgan, B.A., S.C. Institute, and S.S.A. Centre, Concise Guide to the Structural De- sign of Stainless Steel. 1993: Steel Construction Institute.

[18] International, A.S.M., A.S.M International, Metals Handbook, . Ninth edition ed. Vol.

[19] 13. 1987: Corrosion (ASM Handbook).

[20] Schmitt, G. and M. Horstemeier, Fundamental Aspects of CO2 Metal Loss Corrosion Part II: Influence of Different Parameters on CO2 Corrosion Mechanisms. 2006, NACE International.

[21] Charng, T.L., F., Review of corrosion causes and corrosion control in a technical fa- cility. 1982: United States.

[22] Dugstad, K.V.a.A., Film Covered Corrosion, Film Breakdown and Pitting Attack of Carbon Steels in Aqueous CO2 Environments. Corrosion Analysis Network, 1988: p. 1 - 18.

[23] corrosion in oil and gas production. J. S. Smart, III. CORROSION 90/10, NACE, Houston, TX. Per Copy$, 1990.

[24] S.Nesic, J.P.a., Erosion–Corrosion in Single- and Multiphase Flow. 2011, in Uhlig's Corrosion Handbook: John Wiley & Sons, Inc., Hoboken, NJ, USA. .

[25] Venkatesh, E.S., Erosion Damage in Oil and Gas Wells. Society of Petroleum Engi- neers.

[26] Schmitt, G.A., et al., Understanding Localized CO2 Corrosion of Carbon Steel from Physical Properties of Iron Carbonate Scales. NACE International.

[27] Lillard, R.S., et al., Using Local Electrochemical Impedance Spectroscopy to Exam- ine Coating Failure.

[28] Dugstad, A.L., L and Videm, K, Parametric study of CO2 corrosion of carbon steel

[29] NACE International, Houston, TX., 1995.

[30] Nesic, S., et al., Mechanistic Modeling for CO2 Corrosion with Protective Iron Carbonate Films. NACE International.

[31] Sontvedt, E.E.a.T., Effect of Flow on CO2 Corrosion Rate in Real and Synthetic For-

mation Waters. Corrosion Analysis Network, 1983: p. 1-40.

[32] Waard, C.d., U. Lotz, and D.E. Milliams, Predictive Model for CO2 Corrosion Engineering in Wet Natural Gas Pipelines. CORROSION, 1991. 47(12): p. 976-985.

[33] WAARD, C.D. and D.E. MILLIAMS, Carbonic Acid Corrosion of Steel. CORROSION, 1975. 31(5): p. 177-181.

[34] Halvorsen, A.M. and T. Sontvedt, CO2 Corrosion Model for Carbon Steel Including Wall Shear Stress Model for Multiphase Flow and Limits for Production Rate to Avoid Mesa Attack. NACE International.

[35] STANDARD, N., CO2 corrosion rate calculation model. 2005.

[36] Garsany, Y., D. Pletcher, and B.M. Hedges, The Role of Acetate in CO2 Corrosion of Carbon Steel: Has the Chemistry Been Forgotten? NACE Inter